RESEARCH ARTICLE

WILEY

Piperazin incorporated Schiff Base derivatives: Assessment of in vitro biological activities, metabolic enzyme inhibition properties, and molecular docking calculations

Arif Mermer[1,2] | Burak Tüzün[3] | Sevgi Durna Daştan[4] | Ümit M. Koçyiğit[5] | Feyza Nur Çetin[5] | Özge Çevik[6]

[1]Experimental Medicine Application & Research Center, Validebağ Research Park, University of Health Sciences, Istanbul, Türkiye

[2]Department of Biotechnology, University of Health Sciences, Istanbul, Türkiye

[3]Plant and Animal Production Department, Technical Sciences Vocational School of Sivas, Sivas Cumhuriyet University, Sivas, Turkey

[4]Department of Biology, Faculty of Science, Sivas Cumhuriyet University, Sivas, Turkey

[5]Department of Basic Pharmaceutical Sciences, Sivas Cumhuriyet University, Sivas, Turkey

[6]Department of Biochemistry, Adnan Menderes University, Aydın, Turkey

Correspondence

Arif Mermer, Experimental Medicine Application and Research Center, University of Health Sciences, 34662, Istanbul, Turkey. Email: arif.mermer@sbu.edu.tr

Burak Tüzün, Plant and Animal Production Department, Technical Sciences Vocational School of Sivas, Sivas Cumhuriyet University, 58140, Sivas, Turkey. Email: theburaktuzun@yahoo.com

Funding information

Scientific Research Project Fund of Sivas Cumhuriyet University, Grant/Award Number: RGD-020

Abstract

The cytotoxic activities of the compounds were determined by the 3-(4, 5-dimethylthiazolyl-2)-2,5-diphenyltetrazolium bromide (MTT) method in human breast cancer (MCF-7), human cervical cancer (HeLa), and mouse fibroblast (L929) cell lines. The compounds **MAAS-5** and four modified the supercoiled tertiary structure of pBR322 plasmid DNA. **MAAS-5** showed the highest cytotoxic activity in HeLa, MCF-7, and L929 cells with IC50 values of 16.76 ± 3.22, 28.83 ± 5.61, and $2.18 \pm 1.22\,\mu M$, respectively. **MAAS-3** was found to have almost the lowest cytotoxic activities with the IC50 values of 93.17 ± 9.28, 181.07 ± 11.54, and $16.86 \pm 6.42\,\mu M$ in HeLa, MCF-7, and L929 cells respectively at 24 h. Moreover, the antiepileptic potentials of these compounds were investigated in this study. To this end, the effect of newly synthesized Schiff base derivatives on the enzyme activities of carbonic anhydrase I and II isozymes (human carbonic anhydrase [hCA] I and hCA II) was evaluated spectrophotometrically. The target compounds demonstrated high inhibitory activities compared with standard inhibitors with K_i values in the range of 4.54 ± 0.86–15.46 ± 8.65 nM for hCA I (K_i value for standard inhibitor = 12.08 ± 2.00 nM), 1.09 ± 0.32–29.94 ± 0.82 nM for hCA II (K_i value for standard inhibitor = 18.22 ± 4.90 nM). Finally, the activities of the compounds were compared with the Gaussian programme in the B3lyp, HF, M062X base sets with 6-31++G (d,p) levels. In addition, the activities of five compounds against various breast cancer proteins and hCA I and II were compared with molecular docking calculations. Also, absorption, distribution, metabolism, excretion, and toxicity analysis was performed to investigate the possibility of using five compounds as drug candidates.

KEYWORDS

cell culture, density functional theory, Enzyme Inhibition, molecular docking, Schiff base

1 | INTRODUCTION

Cancer treatments often damage healthy cells and tissues. In fact, each type of treatment has significant and varied side effects, which basically depend on the type and extent of the treatment and are not the same for everyone and can even vary from one treatment to the next in the same person. While most people who undergo chemotherapy lose their hair, other side effects vary depending on the type of drug. For this reason, research into new chemo-therapeutic drugs with fewer side effects than the chemotherapeutic

agents used in treatment is a major focus of cancer research.[1] Breast cancer is the most common malignancy in women. Because of its major impact on the population, this disease represents a critical public health problem that requires further research at the molecular level to define its prognosis and specific treatment.[2,3] Basic research is needed to accomplish this task, and this involves cell lines, as they can be widely used in many aspects of laboratory research and, in particular, as in vitro models in cancer research.[4] In the years since HeLa cells were isolated, they have underpinned advances in most areas of medical research. HeLa cells have become the most widely used human cell line in biological research and have been critical to many biomedical applications. L929, mouse fibroblast cells, are widely used to study oxidative stress-induced cytotoxicity.[5]

CA (carbonate hydrolyase, EC 4.2.1.1) is a metalloenzyme found in many tissues that catalyses the reversible hydration of carbon dioxide to bicarbonate. It contains zinc (Zn^{2+}) ions in its active site.[6-8] Carbonic anhydrases are classified into four categories based on their location in the body, with at least 16 different isoforms ranging from CA I to CA XVI. The CA isoenzymes human carbonic anhydrase (hCA) I and hCA II inhibitors are also used as active ingredients in painkillers and diuretics to treat cancer, epilepsy, osteoporosis, hypertension, and eye problems, especially hCA II inhibitors (glucoma).[8-10] Drugs that inhibit CA isoenzymes can also have negative side effects. New alternative CA inhibitors have recently been the focus of exploratory research due to the plethora of adverse effects.[10-14] Studies have revealed the catalytic methods of CA isoenzyme inhibition, the distribution of these isoenzymes in different tissues and their critical activities in these tissues.[12-16] As a result, the inhibitory mechanisms of CA isoenzymes are crucial for the development of novel drugs.

Theoretical calculations are now very common and have evolved with technology. Technological developments have improved computers, and the development of computers has led to faster and more reliable theoretical calculation programs.[17,18] The most important of these theoretical calculation methods are density functional theory (DFT) calculations and molecular docking. In the calculations made, the molecules were calculated at the level of B3lyp, HF, and M062X method with 6-31++g(d,p) basis set. However, the activity of the molecules against different breast cancer proteins (PDB ID: 1JNX and 1A52)[19,20] and hCA I and II (PDB ID: 2CAB and 5AML)[21] was investigated. Absorption, distribution, metabolism, excretion, and toxicity (ADME/T) analysis was also performed to investigate the drug properties of the molecules in this study.

In this study, we aimed to determine the antioxidant or oxidant level-modifying properties of the compounds **MAAS 3–7** in three cell lines, the antimicrobial activities on four different microbial strains and define the cytotoxicity of these compounds on two different cancer cell lines (MCF-7 and HeLa) and one healthy cell line. The L929 cell line consisting of mouse fibroblast cells was used in our study to compare the effects of the compounds used on healthy cells. Furthermore, we report a brief overview of the ability of these compounds to modify the Form I and II bands of pBR322 plasmid DNA with electrophoretic mobility.

2 | MATERIALS AND METHODS

2.1 | Materials and instrumentation

All chemicals and solvents were purchased from Sigma Aldrich-Merck. Reactions were followed by thin-layer chromatography (TLC) on silica gel 60 F254 aluminum sheets. Fourier transform infrared spectroscopy (FTIR) spectra were recorded using a ThermoFisher Scientific Nicolet IS50 FTIR spectrometer. ^{1}H-NMR and ^{13}C-NMR (APT) spectra were recorded on Bruker Avance II 400 MHz NMR spectrometer (chemical shift in ppm downfield from tetramethylsilane as an internal reference). The mass spectra were achieved at a matrix-assisted laser desorption ionization–time-of-flight mass spectrometry (MALDI-TOF/MS) (Bruker, Ultraflextreme). The compounds **1** and **2** are known and synthesized by previously reported method.[22]

2.1.1 | General procedure for the synthesis of compounds (MAAS 3–7)

A mixture of compound **2** (10 mmol) and substituted aromatic aldehyde (10 mmol) in ethanol in the presence of catalytic amount glacial acetic acid was refluxed for 6–8 h. After evaporating the solvent under reduced pressure, a solid was obtained. The obtained compound was recrystallized from an appropriate solvent to afford the desired product.

2-[4-(4-methoxyphenyl)piperazin-1-yl]-N'-[(E)-(4-nitrophenyl) methylidene]aceto hydrazide (MAAS-3)

Yellowish solid. Recrystallized from MeOH. FT-IR (v_{max}, cm^{-1}): 3243.73 (NH), 3044.68 (ar–CH), 1685.52 (C=O), 1602.61 (C=N). ^{1}H NMR (dimethylsulfoxide [DMSO]-d_6, δppm): 2.61–2.72 (m, 4H, 2CH$_2$), 2.99–3.06 (m, 4H, 2CH$_2$), 3.16 (s, 2H, CH$_2$), 3.66 (s, 3H, OCH$_3$), 6.79 (dd, 2H, J = 1.2 Hz, arH), 6.87 (dd, 2H, J=9.2 Hz, arH), 7.91 (q, 2H, J_1=6.8 Hz, J_2=6.8 Hz, arH), 8.26 (q, 2H, J_1=6.8 Hz, J_2=6.8 Hz, arH), 8.42 (s, 1H, CH), 11.49 (s, 1H, NH). ^{13}C NMR (DMSO-d_6, δppm): 49.85, 50.11, 53.17, 53.35, 55.61, 60.95, 114.67, 117.75–117.79 (d, J=4.0 Hz), 124.50, 128.08, 128.37, 141.09, 145.09, 145.80, 148.24, 153.31, 166.57. MALDI-TOF-MS: 395.17513 ([M-2]$^+$).

N'-[(E)-(4-chlorophenyl)methylidene]-2-[4-(4-methoxyphenyl) piperazin-1-yl] acetohydrazide (MAAS-4)

White solid. Recrystallized from MeOH. FT-IR (v_{max}, cm^{-1}): 3433.03 (NH), 3051.75 (ar–CH), 1676.12 (C=O), 1592.48 (C=N). ^{1}H NMR (DMSO-d_6, δppm): 2.61–2.69 (br, d, 4H, 2CH$_2$), 3.02 (d, 4H, J=16.0 Hz, 2CH$_2$), 3.12 (s, 2H, CH$_2$), 3.66 (s, 3H, OCH$_3$), 6.83 (dd, 4H, J=4.0 Hz, arH), 7.48 (d, 2H, J=6.8 Hz, arH), 7.67 (t, 2H, J=8.0 Hz, arH), 8.30 (s, 1H, CH), 11.24 (s, 1H, NH). ^{13}C NMR (DMSO-d_6, δppm): 49.85, 50.10, 53.21, 53.35, 55.60, 60.96, 114.67, 117.74-117.79 (d, J=5.0 Hz), 128.79, 129.08, 129.34, 133.69, 141.95, 145.80, 145.92, 146.23, 153.31, 166.16. MALDI-TOF-MS: 386.11248 ([M]$^+$).

N'-[(E)-(4-fluorophenyl)methylidene]-2-[4-(4-methoxyphenyl) piperazin-1-yl] acetohydrazide (MAAS-5)

White solid. Recrystallized from EtOAc. FT-IR (v_{max}, cm^{-1}): 3435.90 (NH), 3019.18 (ar–CH), 1678.35 (C=O), 1597.94 (C=N). ^{1}H NMR (DMSO-d_6, δppm): 2.61–2.69 (br, d, 4H, 2CH$_2$), 3.02 (d, 4H, J=16.0 Hz, 2CH$_2$), 3.12 (s, 2H, CH$_2$), 3.66 (s, 3H, OCH$_3$), 7.14 (dd, 4H, J=8.0 Hz, arH), 7.48 (d, 2H, J=4.0 Hz, arH), 7.67 (t, 2H, J=8.0 Hz, arH), 8.38 (s, 1H, CH), 11.04 (s, 1H, NH). ^{13}C NMR (DMSO-d_6, δppm): 49.85, 50.11, 53.17, 53.35, 56.55, 62.03, 116.35, 119.25, 125.47, 128.37, 131.81, 142.05, 144.38, 151.80, 159.17-162.04 (d_{C-F}=287.0 Hz), 167.68. MALDI-TOF-MS: 370.18679 ([M]$^+$).

N'-[(E)-(4-methoxyphenyl)methylidene]-2-[4-(4-methoxyphenyl) piperazin-1-yl] acetohydrazide (MAAS-6)

White solid. Recrystallized from EtOAc. FT-IR (v_{max}, cm^{-1}): 3435.85 (NH), 3063.26 (ar–CH), 1678.04 (C=O), 1599.73 (C=N). ^{1}H NMR (DMSO-d_6, δppm): 2.65–2.81 (m, 4H, 2CH$_2$), 2.98–3.05 (m, 4H, 2CH$_2$), 3.23 (s, 2H, CH$_2$), 3.65 (s, 3H, OCH$_3$), 3.81 (s, 3H, OCH$_3$), 6.59 (d, 2H, J=4.0 Hz, arH), 6.70 (d, 2H, J=8.0 Hz, arH), 6.93 (d, 2H, J=8.0 Hz, arH), 7.16 (d, 2H, J=4.0 Hz, arH), 8.46 (s, 1H, CH), 11.39 (s, 1H, NH). ^{13}C NMR (DMSO-d_6, δppm): 49.85, 50.36, 52.86, 53.15, 55.61, 56.04, 114.32, 116.21, 127.14, 129.12, 143.39, 148.66, 152.79, 160.14, 165.36. MALDI-TOF-MS: 382.18698 ([M]$^+$).

N'-[(E)-(4-bromophenyl)methylidene]-2-[4-(4-methoxyphenyl) piperazin-1-yl] acetohydrazide (MAAS-7)

White solid. Recrystallized from EtOH. FT-IR (v_{max}, cm^{-1}): 3439.91 (NH), 3019.01 (ar–CH), 1679.15 (C=O), 1598.05 (C=N). ^{1}H NMR (DMSO-d_6, δppm): 2.60–2.71 (m, 4H, 2CH$_2$), 2.99–3.06 (m, 4H, 2CH$_2$), 3.12 (s, 2H, CH$_2$), 3.66 (s, 3H, OCH$_3$), 6.79 (dd, 2H, J=6.8 Hz, arH), 6.86 (dd, 2H, J=2.8 Hz, arH), 7.62 (s, 2H, arH), 7.71 (d, 1H, J=8.4 Hz, arH), 7.81 (d, 1H, J=8.0 Hz, arH), 8.28 (s, 1H, CH), 11.25 (s, 1H, NH). ^{13}C NMR (DMSO-d_6, δppm): 49.85, 50.08, 53.20, 53.34, 55.61, 60.95, 114.67, 117.79, 129.03, 129.32, 130.65, 132.25, 132.46, 145.80, 146.32, 161.18, 166.17. MALDI-TOF-MS: 431.15206 ([M+1]$^+$).

2.2 | Cell culture growing and proliferation assay

Mouse fibroblast cell (L929), Human cervical cancer cell (HeLa), Human breast adenocarcinoma cell (MCF7) lines were used while the L929 cell line is a healthy cell line is generally used for control purposes in studies. All cell lines were cultured in 25 cm^2 flasks (Corning-Sigma-Aldrich) in an incubator at 37°C, containing 5% CO$_2$ and 95% moisture, in Dulbecco's modified Eagle's medium (DMEM) containing 10% fetal Bovine serum (FBS), Penicilin-Streptomycin (100 U/mL penicillin, and 100 µg/mL streptomycin), L-Glutamine and NaHCO$_3$. While growing cells were passaged, Trypsin-EDTA was added and kept in a CO$_2$ oven for about 1 min. The medium was then added and the cells were collected in a Falcon tube and centrifuged at 1000 rpm for 5 min at room temperature. The supernatant was discarded and the precipitated pellet was suspended in medium,

counted, and plated into culture plates. To determine the effects of target compounds on cell viability, cells were plated in 96-well plates (1 x 10^4 cells/well) for 24 h.[23] The in vitro cytotoxicity of the extract was assessed using the 3-(4,5-dimethylthiazolyl-2)-2,5-diphenyltetrazolium bromide (MTT) colourimetric assay. The MTT assay is used to measure cellular metabolic activity as an indicator of cell viability, proliferation, and cytotoxicity. This colorimetric assay is based on the reduction of a yellow tetrazolium salt (MTT) to purple formazan crystals by metabolically active cells. The various concentrations of the compounds (0.1–100 µM), prepared in 1% DMSO-growth medium, were added onto the cell culture in 96-well plate for 24 h. Each dilution concentration was performed in triplicate. After 24 h, 10 µL of 12 mM MTT (Vybrant, Invitrogen) solution was added to wells and incubated inside a 5% CO$_2$ store at 37°C for 4 h. To determine the cytotoxic activity of the cells, the absorbance of violet color that occurred at the end of fourth hour was measured at 570 nm in a microplate reader (Epoch). As a result of MTT experiments, IC50 values were calculated using the Graphpad program and then graphs were generated. The selectivity index (SI) of compounds was calculated by obtaining the ratio of IC50 in the healthy cell line/IC50 in the cancer line.

2.3 | Morphological visualization of cells

The synthesized compounds were added to each of the cells. The morphology of the cells after the application of the 10 µM compound dose was examined under the microscope (ZEISS Axio).

2.4 | Antimicrobial activity assay

Antimicrobial activity values were determined by the minimum inhibition concentration (MIC) of the compounds **MAAS 3–7** against microorganisms with the "Microdilution Broth Method".[24] Microorganism strains used in the study: *Staphylococcus aureus*, *Pseudomonas aeruginosa*, *Escherichia coli*, *Candida albicans*. The antimicrobial activity assays for these compounds were performed according to the previously reported method.[25]

2.5 | Antioxidant activity assays

Following application, phosphate buffer (pH =7.4; 50 mM) was first added to the cell samples at a rate of 1/9 (v/v) and homogenized in a refrigerated environment for biochemical analysis. To determine changes in the total antioxidant-oxidant load of the cell lines after administration of the **MAAS 3–7** compounds at 10 µM, cells were plated on 24-well plates (1 x 10^4 cells/well) for 24 h. Then, phosphate buffer (pH=7.4; 50 mM) was added to the cell samples at a rate of 1/9 (v/v) and homogenization was performed in a refrigerated environment for biochemical analysis. After homogenization, the homogenates were centrifuged at 3000 rpm for 15 min.

The supernatants obtained from centrifugation were used for biochemical analyses.[26] After the homogenate was filtered, the manufacturer's protocol was followed according to the procedure of the Total antioxidant levels/total oxidant levels (TAS/TOS) kits. TAS, TOS, and oxidative stress index (OSI) were determined in triplicate experiments using commercially available Rel Assay Diagnostic kits.[27] Trolox was used as a standard for TAS analyses and hydrogen peroxide for TOS analyses. The OSI was calculated using the following equation:

$$OSI \text{ (Arbitrary Unit)} = \frac{TOS, \text{ μmol } H_2O_2 \text{ equiv/L}}{TAS, \text{ mmol Trolox equiv/L X 10}}.$$

2.6 | The compounds and pBR322 plasmid DNA interaction assay

The interaction of the compounds **MAAS 3–7** with pBR322 plasmid DNA was studied by agarose gel (%1.5) electrophoresis according to the protocol modified by Bogatarkan et al.[28] The 40 μL aliquots of increasing concentrations of the complexes, ranging from 1.0 to 100 μM, were added to 1 μL of plasmid DNA (concentration of 0.5 μg/mL) in a buffer solution containing TE buffer (pH = 7.4). The samples were incubated at 37°C for 24 h in the dark, and then 10 μL aliquots of drug–DNA mixtures were mixed with loading buffer and loaded into 1.5% agarose gel with ethidium bromide. Electrophoresis was carried out TBE buffer (pH = 8.0) for 5 h at 40 V. The gel was then viewed with a UV transilluminator, and the image was captured as a photograph (Syngene).

2.7 | Statistical analysis

SPSS 23.0 (IBM Corporation) program was used for statistical data analysis. The data were analyzed at 95% confidence level, and if the p value was less than 0.05, it was considered significant. The results are given as mean ± SD. The statistical significance levels of the doses are given on the figures (*$p < 0.05$, ** $p < 0.01$ and ***$p < 0.001$, ****$p < 0.0001$).

2.8 | Enzyme studies

The inhibitory effects of novel piperazine-incorporated Schiff base derivatives (**MAAS 3–7**) on the esterase activity of hCAs were evaluated using the Verpoorte method. The principle of the method: The carbonic anhydrase enzyme hydrolyses p-nitrophenyl acetate, which is used as a substrate, to p-nitrophenol or p-nitrophenolate, which absorbs at 348 nm. Both p-nitrophenol and its salt, p-nitrophenolate, absorb at 348 nm. Therefore, whether or not the H+ in the phenol group dissociates does not affect the measurement.[29–32] As p-nitrophenyl acetate has very little absorbance at this wavelength, it is used blind. The changes in absorbance of the cuvette contents prepared according to the appropriate procedure are measured in 3 min. IC50 and K_i values are calculated from the results obtained.

2.9 | Theoretical methods

It is used to compare both chemical and biological activities of the compounds with theoretical calculations. Many quantum chemical parameters are calculated when examining the chemical properties of compounds. Each parameter gives information about the different properties of compounds. Gaussian09 RevD.01, GaussView 6.0[33,34] are used to calculate these parameters. B3LYP, HF, M06-2x[35-37] level of molecules with the 6-31++G (d,p) basis set calculations were performed using these programs. As a result of these calculations, many quantum chemical parameters were calculated, which are HOMO (Highest Occupied Molecular Orbital), LUMO (Lowest Unoccupied Molecular Orbital), ΔE (HOMO–LUMO energy gap), chemical potential (μ), electrophilicity (ω), chemical hardness (η), global softness (σ), nucleophilicity (ε), dipole moment, energy value.[38-40] These parameters have been calculated using the following equations:
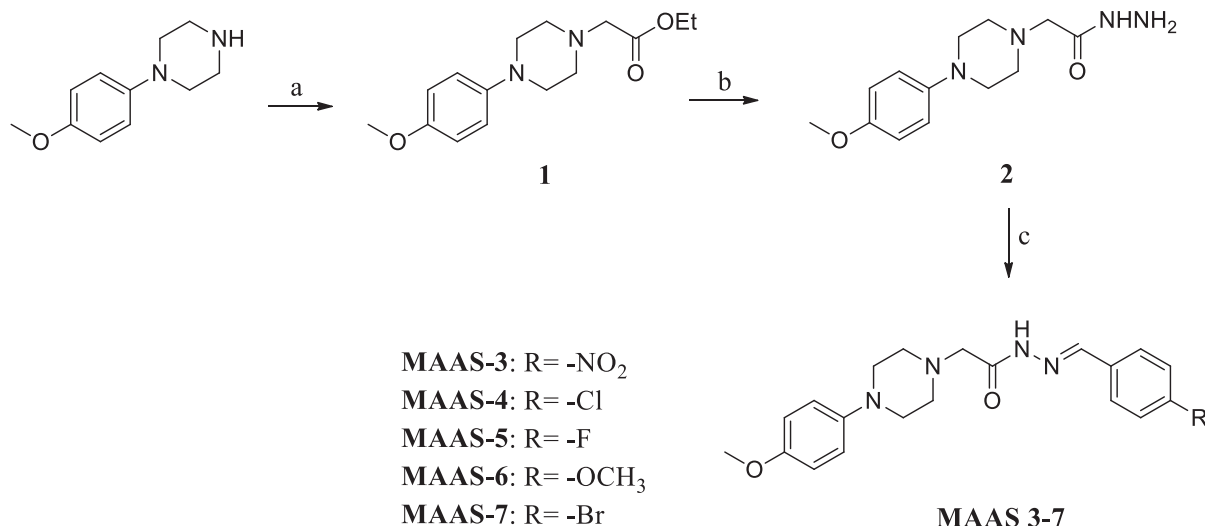
$$\chi = -\left(\frac{\partial E}{\partial N}\right)_{\upsilon(r)} = \frac{1}{2}(I + A) \cong -\frac{1}{2}(E_{HOMO} + E_{LUMO}),$$

$$\eta = -\left(\frac{\partial^2 E}{\partial N^2}\right)_{\upsilon(r)} = \frac{1}{2}(I - A) \cong -\frac{1}{2}(E_{HOMO} - E_{LUMO}),$$

$$\sigma = 1/\eta \quad \omega = \chi^2/2\eta \quad \varepsilon = 1/\omega.$$

To examine the biological activities of the synthesized target compounds, their inhibitory activities against various cancer proteins were studied. For this purpose, the Maestro Molecular modelling platform (version 12.8) by Schrödinger[41] was used. The protein preparation module was used to prepare proteins,[42] the LigPrep module[43] was used for the preparation of compounds, and the Glide ligand docking module[44] was benefited to interact between the prepared compounds and proteins. However, the study was carried out using ADME/T analysis that is performed via The Qik-prop module,[45] so that the studied compounds could be used as drug candidates.

3 | RESULTS

3.1 | Chemistry

In the present study, five novel piperazine-incorporated Schiff base derivatives **MAAS 3–7** were synthesized for the first time (Scheme 1). The compound ethyl 2-[4-(4-methoxyphenyl)piperazin-1-yl]acetate (**2**) and its corresponding hydrazide compound were achieved according to the previously reported method.[22] The obtained hydrazide compound (**3**) was then treated with aromatic aldehydes containing electron-donating or withdrawing substituents such as nitro, fluorine, chloride, bromide, and methoxy. The reaction was successfully carried out in high yields (88%–94%) in the presence of

MAAS-3: R= -NO$_2$
MAAS-4: R= -Cl
MAAS-5: R= -F
MAAS-6: R= -OCH$_3$
MAAS-7: R= -Br

MAAS 3-7

SCHEME 1 Synthetic pathway for compounds MAAS 3–7. a: BrCH$_2$COOEt, K$_2$CO$_3$, Acetone; b: NH$_2$NH$_2$.H$_2$O, EtOH; c: RCHO, EtOH, AcOH.

TABLE 1 Comparison of IC50 values of compounds MAAS 3-7 in cell lines.

IC50 (μM±SD)			
Compounds	HELA cell line	MCF7 cell line	L929 cell line
MAAS-3	93.17 ± 9.28 μM	181.07 ± 11.54 μM	16.86 ± 6.42 μM
MAAS-4	25.91 ± 4.81 μM	16.77 ± 3.19 μM	2.73 ± 1.43 μM
MAAS-5	16.76 ± 3.22 μM	28.83 ± 5.61 μM	2.18 ± 1.22 μM
MAAS-6	41.5 ± 8.98 μM	227 ± 16.72 μM	13.57 ± 3.09 μM
MAAS-7	38.82 ± 6.12 μM	252.7 ± 18.23 μM	7.79 ± 3.03 μM

catalytic amounts of glacial acetic acid based on previously reported methods.[46,47]

The molecular characterization of the synthesized compounds was confirmed by spectroscopic methods such as FT-IR, ^{1}H NMR, ^{13}C NMR (APT), and MALDI-TOF/MS. In the FT-IR spectra, the disappearance of the −NH$_2$ vibrational band at about 3200 cm^{-1} belonging to the hydrazide group in compound **2**, the shift of the band attributed to the carbonyl group and the vibrational bands showing the formation of imine bonds in the region of 1592.46 and 1602.01 cm^{-1} confirmed the structures of the synthesized compounds. One of the most prominent signals in the ^{1}H NMR spectra, proving the molecular structures, was that the proton (−N=CH) signal for the imine group was observed in the range of 8.28–8.46 ppm. Furthermore, the disappearance of the amine (−NH$_2$) protons of the hydrazide compound was another important piece of evidence. In the ^{13}C NMR (APT) spectra, the carbon signal related to the imine group (−N=CH) resonated between 144.38 and 148.66 ppm. Similarly, the synthesized piperazine Schiff base derivatives demonstrated their respective *m/z* value peaks according to the molecular mass of the compounds.

3.2 | Cell growth and antiproliferative activity results

The cytotoxic activities of the compounds were evaluated and the results are shown in Table 1 and Figure 1. The percentages of cell survival after administration of the compounds **MAAS 3–7** were calculated and compared with each other. The IC50 doses of the compounds applied to the cells were found to be more effective in L929 and HeLa cells. Compound **MAAS-4** showed the highest cytotoxic activity with an IC50 dose of 16.77 ± 3.19 μM among the compounds against MCF-7 cells. Compound **MAAS-5** exhibited the highest cytotoxic activity with an IC50 dose of 16.76 ± 3.22 μM on HeLa cells. The **MAAS-5** and **MAAS-4** compounds were also found to cause the highest cytotoxic activity in L-929 cells at IC50 value of 2.18 ± 1.22 μM and 2.73±1.43 μM, respectively. The target compounds demonstrated different levels of cytotoxic activity on the L929 cell line. The lowest IC50 values were obtained for the compounds **MAAS-3**, **MAAS-6**, and **MAAS-7** in MCF-7 cell line with the 181.07 ± 11.54, 227 ± 16.72, and 252.7 ± 18.23 μM doses, respectively.
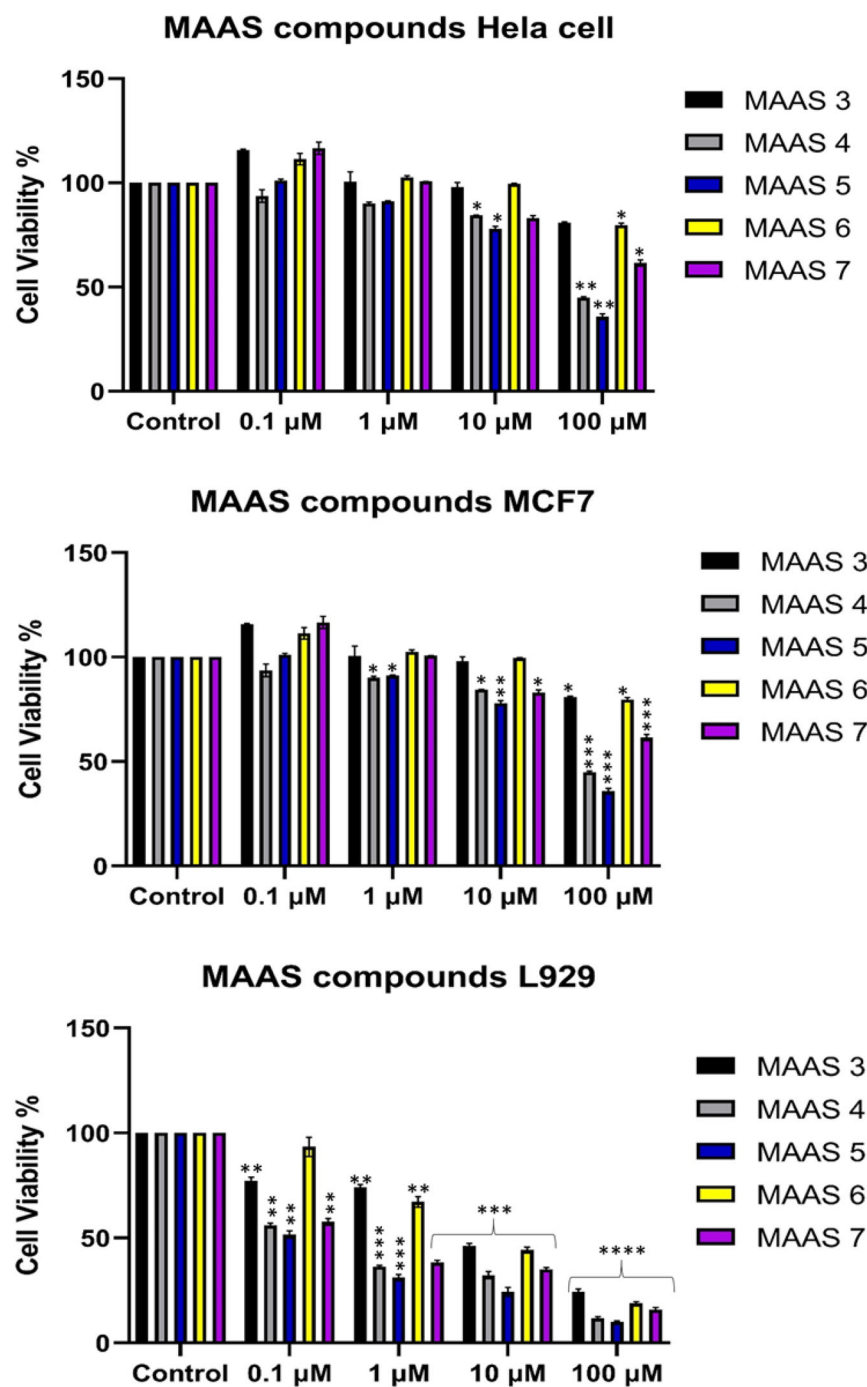
FIGURE 1 Determination of the cytotoxic activity of the **MAAS 3–7** compounds in MCF-7, HeLa, and L929 cell lines. Activities of compounds after 24-h incubation at concentrations ranging from 0.1 to 100 μM (*$p < 0.05$, **$p < 0.01$, ***$p < 0.001$, and ****$p < 0.0001$).

TABLE 2 The selectivity index (SI) of the MAAS 3–7 compounds at 24 h treatment.

Selectivity Index	L929/MCF 7	L929/HeLa
MAAS-3	0.093 ± 0.556	0.181 ± 0.692
MAAS-4	0.163 ± 0.448	0.105 ± 0.297
MAAS-5	0.076 ± 0.217	0.130 ± 0.379
MAAS-6	0.060 ± 0.185	0.327 ± 0.344
MAAS-7	0.031 ± 0.166	0.201 ± 0.495

It was also clear that compounds **MAAS-5**, **MAAS-4**, and **MAAS-7** exhibited the highest cytotoxic activity with IC50 doses much lower than 10 μM on only the L929 cell line. The other compounds generally exhibited IC50 values higher than 10 μM on the cell lines given in Table 1. As a matter of fact, it is accepted by the NCBI Cancer Institute that compounds with IC50 values above 10 μM do not have a significant cytotoxic effect, but if the IC50 value of compounds is between 10 and 100 μM, they are considered to have a moderate cytotoxic effect. Therefore, advanced anticancer analyses were not conducted because the IC50 values of compounds on cell
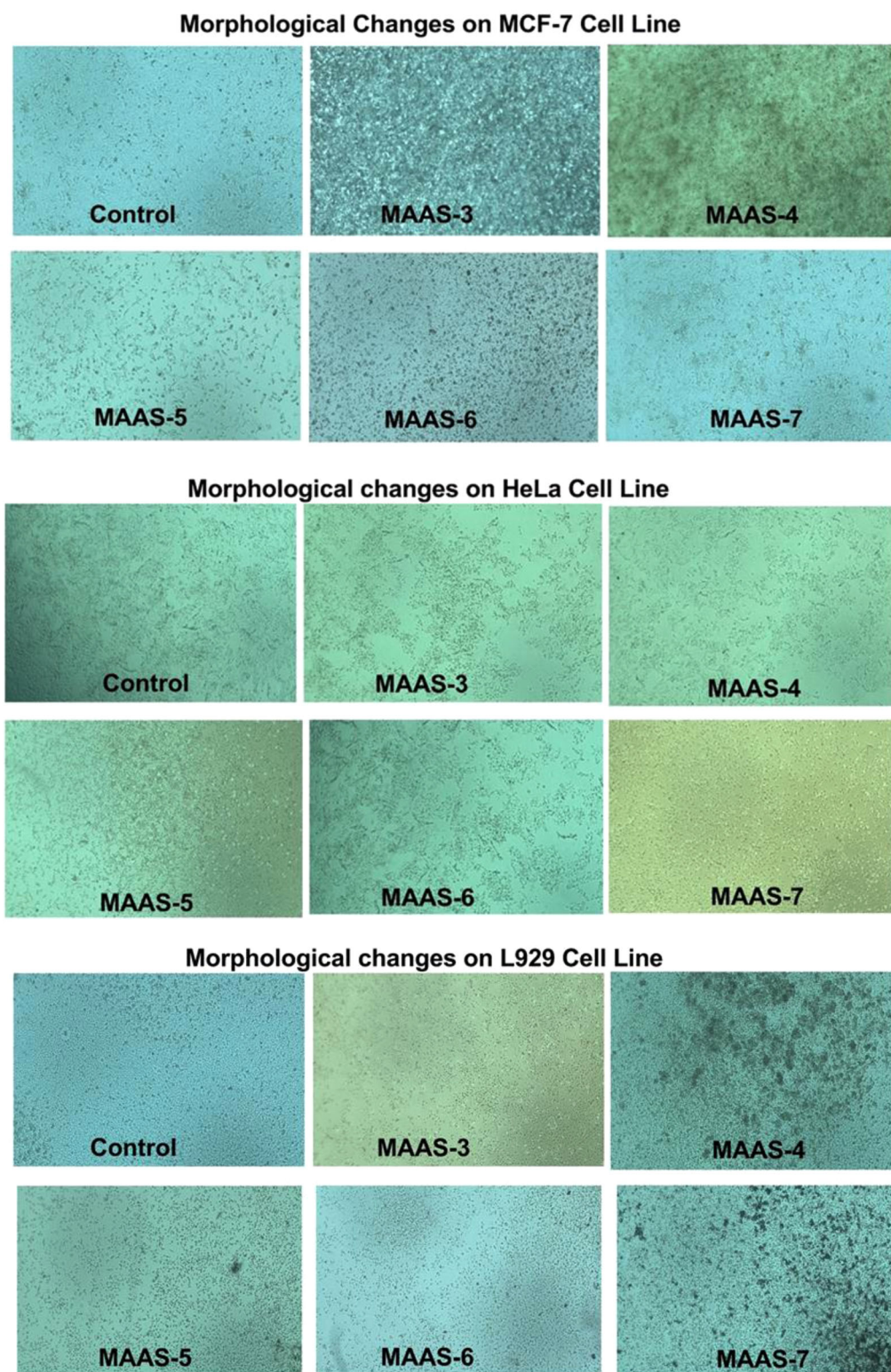
FIGURE 2 Morphological changes of cells after 24 h of incubation with 10 µM dose of compounds **MAAS 3–7**.

lines were above the 10 µM threshold. However, by using IC50 values, it is possible to compare the compounds on three cell lines to determine which cell lines are more affected by using the selectivity index (SI) in Table 2.

Almost all the SI values of these compounds were very low and close to each other. The results suggest that these compounds have almost the same cytotoxic activities on both MCF7 and HeLa cancer cell lines. Morphological analyses were performed 24 h after the administration of

TABLE 3 MIC values on some microbial strains of the MAAS 3–7 compounds.

Value units (mg.mL^{-1})	Escherichia coli	Staphylococcus aureus	Pseudomonas aeruoginosa	Candida albicans
MAAS 3	>5	>5	>5	>5
MAAS 4	0.31	0.16	0.16	0.31
MAAS 5	0.16	0.16	0.16	0.31
MAAS 6	>5	>5	1.35	1.35
MAAS 7	0.63	0.63	0.63	0.31

TABLE 4 TAS, TOS, and OSI values from MCF-7, HeLa, and L929 cell lines that are treated with the compounds MAAS 3–7 for 24 h.

Mean ± S.E.		MCF-7	HeLa	L929
TAS values	Control	0.408 ± 0.006	0.502 ± 0.011	0.398 ± 0.009
	MAAS-3	0.417 ± 0.014	0.516 ± 0.027	0.419 ± 0.059
	MAAS-4	0.458 ± 0.022	0.561 ± 0.033	0.442 ± 0.081
	MAAS-5	0.475 ± 0.030	0.578 ± 0.028	0.456 ± 0.073
	MAAS-6	0.421 ± 0.023	0.529 ± 0.065	0.423 ± 0.094
	MAAS-7	0.431 ± 0.025	0.549 ± 0.091	0.430 ± 0.047
TOS values	Control	0.744 ± 0.025	0.838 ± 0.044	0.713 ± 0.026
	MAAS-3	0.751 ± 0.054	0.854 ± 0.078	0.744 ± 0.098
	MAAS-4	0.816 ± 0.081[a]	0.890 ± 0.056[b]	0.798 ± 0.094[c]
	MAAS-5	0.829 ± 0.049[a]	0.912 ± 0.075[b]	0.817 ± 0.098[c]
	MAAS-6	0.774 ± 0.075	0.869 ± 0.078	0.764 ± 0.071[c]
	MAAS-7	0.798 ± 0.086[a]	0.874 ± 0.090[b]	0.776 ± 0.091[c]
OSI values	Control	0.0182 ± 0.0042	0.1669 ± 0.0040	0.1791 ± 0.0028
	MAAS-3	0.1804 ± 0.0039[d]	0.1664 ± 0.0029	0.1784 ± 0.0017
	MAAS-4	0.1783 ± 0.0037[d]	0.1592 ± 0.0017	0.1812 ± 0.0012
	MAAS-5	0.1752 ± 0.0016[d]	0.1583 ± 0.0027	0.1793 ± 0.0013
	MAAS-6	0.1841 ± 0.0033[d]	0.1640 ± 0.0012	0.1810 ± 0.0008
	MAAS-7	0.1850 ± 0.0034[d]	0.1594 ± 0.0010	0.1804 ± 0.0019

Note: Values are presented as mean±SE; Experiments were made in triplicate.

Abbreviations: OSI, oxidative stress index; TAS, total antioxidant levels; TOS, total oxidant levels.
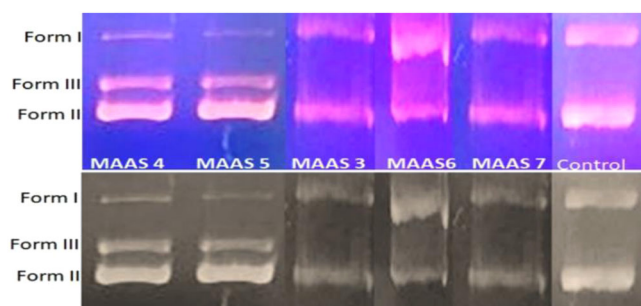

FIGURE 3 Visualization of gel electrophoretic pattern of pBR322 plasmid DNA when incubated with 100 μM concentrations of **MAAS 3–7**. The colorful image is a direct agarose gel electrophoresis image, and the black-colored image is taken from the gel imaging system (SynGene).

the compounds **MAAS 3–7** at a dose of 10 μM to the three cell lines in Figure 2. The compounds **MAAS-5** and **MAAS-4** were found to alter the morphology only of the L929 cells in the cell lines (Figure 2).
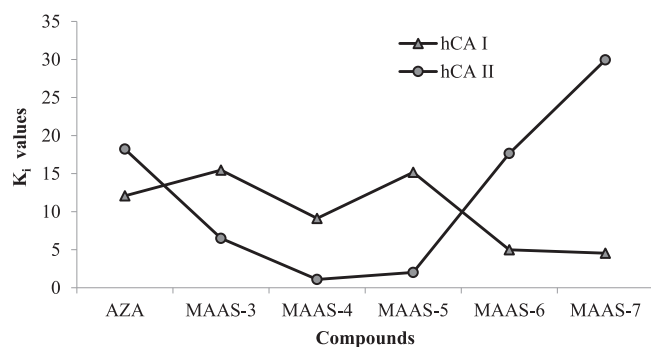
3.3 | Antimicrobial activity results

Antimicrobial activity of the compounds is provided in Table 3. If the MIC values are less than 0.1 mg.mL^{-1} (MIC < 0.1 mg.mL^{-1}), the antimicrobial activity is considered high, and the MIC values are between 0.1 and 0.625 mg.mL^{-1}, these situations indicate the moderate antimicrobial activity. The compounds **MAAS-4**, **5**, and **7** have been found to be moderately effective on the microorganisms used in this study.

TABLE 5 The enzyme inhibition results of novel compounds (MAAS-3–7) against carbonic anhydrase I and II iszoenzymes.

Compounds	IC$_{50}$(µM) hCA I	K$_i$ (µM) r^2	hCA II	r^2	hCA I	hCA II
MAAS-3	0.45	0.9658	0.42	0.8951	6.77 ± 6.08	6.49 ± 1.79
MAAS-4	0.63	0.9839	0.35	0.9210	15.46 ± 8.65	1.09 ± 0.32
MAAS-5	0.60	0.9444	0.80	0.9381	9.12 ± 7.52	2.01 ± 1.06
MAAS-6	0.28	0.9550	0.40	0.8880	4.99 ± 0.09	17.65 ± 13.38
MAAS-7	0.38	0.9517	0.27	0.870	4.54 ± 0.86	29.94 ± 0.82
AZA	12.62	0.9712	19.81	0.9706	12.08 ± 2.00	18.22 ± 4.90

Note: AZA (acetazolamide) was used as a positive control for human carbonic anhydrase I and II isoforms (hCA I and II).

FIGURE 4 K$_i$ values for human carbonic anhydrase I (hCA I) and human carbonic anhydrase II (hCA II) isoenzymes.

The compound **MAAS-3** did not demonstrate any antimicrobial activity. However, it should be noted that a limited number of microorganism strains were used in this study and these tests should be performed on a much larger number of microorganism strains to provide clearer information on the antimicrobial activities of these compounds.

3.4 | Antioxidant activity results

The antioxidant potentials of compounds generally derive from their anti-scavenging activity on reactive oxygen species. Antioxidants eliminate harmful free radical reactions and thus prevent degenerative diseases.[26,27] The TAS values of cells treated with the compounds are found generally high, but they are not statistically significant compared with the control group (p>0.05). Although the antioxidant capacity of the cell cultures treated with the target compounds increased, the differences were found to be insignificant (p > 0.05) in Table 4. When the ability of the test compounds to alter the TOS of cell cultures was evaluated, it was observed that the oxidant level generally increased 24 h after the application of compounds **MAAS-4**, **5**, and **7**. Furthermore, the increases in TOS are statistically significant (p≤0.05) in all the cell lines applied in Table 4.

On the other hand, statistically significant increases in OSI values were observed only in the MCF7 cell line experiments compared with the control group in Table 4. When the test compounds were applied to the cell lines at a dose of 10 µM, statistically significant increases in TOS were observed in general, but it was noted that the compounds statistically increased the OSI only in the MCF-7 cell line. The OSI is expressed as the ratio between the TOS and the total antioxidant level. As for the groups that significantly increased OSI levels compared with the control group, this can be explained by the fact that cellular damage occurs in cell metabolism due to increased formation and levels of lipid peroxidation and reactive oxygen species.

3.5 | Interaction with pBR322 plasmid DNA and compounds

Nowadays, it is accepted that the antineoplastic activity of the drug is based on its interaction with cellular DNA. If the cell cannot remove the DNA damage, by the time the cells die by one of metabolic pathways.[48] In this research, the effect of the compounds **MAAS 3–7** binding on pBR322 plasmid DNA tertiary structure was investigated by their ability to modify the supercoiling of closed circular pBR322 plasmid DNA. There are normally two forms of pBR322 plasmid DNA. Form I is the intact covalently closed circular form and is fast moving. If modification occurs on one chain, the supercoiled form will unwind to generate a slower moving open circular form II. If both double chains are cleaved by any factor, the linear Form III is presented, which migrates between Form I and Form II. Within the scope of this study, pBR322 plasmid DNA was treated with four different doses of compound in the range of 0.1–100 µM at 37°C for 24 h. No interaction between plasmid DNA bands was detected at low doses except for the 100 µM dose. In addition, among the compounds applied at 100 µM dose, only interaction between the compounds **MAAS-4**, **MAAS-5**, and plasmid DNA was observed. In the visualization of these samples (compounds **MAAS-4** and **MAAS-5** at 100 µM concentration), it was seen that the density of the Form I and Form II bands decreased, while the Form III band appeared between two bands on the gel in Figure 3.

This electrophoretic visualization pattern of pBR322 plasmid DNA forms is consistent with previous reports.[49] This situation may

TABLE 6 The calculated quantum chemical parameters of molecules.

	E_{HOMO}	E_{LUMO}	I	A	ΔE	η	μ	χ	$P\dot{i}$	ω	ε	dipol	Energy
B3LYP/6-31g LEVEL													
3	−5.3373	−3.2387	5.3373	3.2387	2.0986	1.0493	0.9530	4.2880	−4.2880	8.7617	0.1141	1.7435	−36741.2574
4	−5.2312	−2.0803	5.2312	2.0803	3.1508	1.5754	0.6348	3.6557	−3.6557	4.2416	0.2358	2.6911	−43682.8105
5	−5.2203	−1.9527	5.2203	1.9527	3.2676	1.6338	0.6121	3.5865	−3.5865	3.9365	0.2540	2.9428	−33876.9416
6	−5.1585	−1.6656	5.1585	1.6656	3.4929	1.7464	0.5726	3.4121	−3.4121	3.3331	0.3000	5.8844	−34291.9555
7	−5.2366	−2.0942	5.2366	2.0942	3.1424	1.5712	0.6365	3.6654	−3.6654	4.2755	0.2339	2.7079	−101141.0300
HF/6-31g LEVEL													
3	−8.8413	0.6389	8.8413	−0.6389	9.4802	4.7401	0.2110	4.1012	−4.1012	1.7742	0.5636	3.8909	−36516.6395
4	−8.7376	0.9203	8.7376	−0.9203	9.6579	4.8290	0.2071	3.9087	−3.9087	1.5819	0.6322	1.2277	−43467.4201
5	−8.7268	0.9219	8.7268	−0.9219	9.6487	4.8243	0.2073	3.9024	−3.9024	1.5783	0.6336	1.3797	−33670.0009
6	−8.4653	0.9483	8.4653	−0.9483	9.4136	4.7068	0.2125	3.7585	−3.7585	1.5006	0.6664	2.9359	−34077.9136
7	−8.7151	0.9149	8.7151	−0.9149	9.6299	4.8150	0.2077	3.9001	−3.9001	1.5795	0.6331	1.1970	−100895.6839
M062X/6-31g LEVEL													
3	−6.7572	−2.0882	6.7572	2.0882	4.6690	2.3345	0.4284	4.4227	−4.4227	4.1894	0.2387	1.5909	−36725.5141
4	−6.9137	−1.0691	6.9137	1.0691	5.8445	2.9223	0.3422	3.9914	−3.9914	2.7259	0.3669	2.4721	−43668.4183
5	−6.9009	−0.9037	6.9009	0.9037	5.9972	2.9986	0.3335	3.9023	−3.9023	2.5392	0.3938	2.6792	−33862.4329
6	−6.8456	−0.6547	6.8456	0.6547	6.1909	3.0955	0.3231	3.7502	−3.7502	2.2717	0.4402	4.3891	−34276.9386
7	−6.9172	−1.0974	6.9172	1.0974	5.8197	2.9099	0.3437	4.0073	−4.0073	2.7593	0.3624	2.4414	−101129.4679

be related to the unwinding of supercoiled DNA to open circular and linear DNA. All the Form I, II, and III bands were observed at high concentrations of only 100 μM of the compounds **MAAS-4** and **MAAS-5** applied to pBR322 plasmid DNA.

3.6 | Carbonic anhydrases inhibition activity results

The study also looked into the possibility of using new piperazine included Schiff base derivatives antiepileptic agents such as pharmaceuticals, which could be an alternative to currently available drugs with a wide range of potential adverse effects. The effect of these newly synthesized piperazine-Schiff base derivatives on the enzyme activity of carbonic anhydrase I and II isoenzymes was evaluated spectrophotometrically for this aim.

An esterase assay technique was used to investigate the inhibitory potentials of the prepared compounds against two physiologically relevant CA isoforms, the slower cytosolic isoform (hCA I) and the faster cytosolic isoenzyme (hCA II). The inhibition data of the compounds against CA I and II isoforms are summarized in Table 5 and Figure 4 (IC50 and K_i values expressed in micromolar (μM)).

All the synthesized compounds were remarkably inhibited both the cytosolic isoforms hCA I (IC_{50} ranging between 0.28 and 0.63 μM) and hCA II (IC_{50} ranging between 0.27 and 0.80 μM). The compounds **MAAS-6** and **MAAS-7** were specified as the best

inhibitors for these isoforms (hCA I and hCA II) with IC_{50} values of 0.28 and 0.20 μM, respectively. It can be said that the methoxy group attached as a substituent in the compound **MAAS-6** increases the inhibitory potential. The significant inhibitory effects of the derivatives against hCA I and hCA II in a range of K_i from 1.09 ± 0.32 to 29.94 ± 0.82 μM in Table 5.

For hCA I, K_i values of acetazolamide (AZA) as positive control and the novel compounds were studied in this study the following order: **MAAS-7**(4.54 ± 0.86 μM) < **MAAS-6** (4.99 ± 0.09 μM) < **MAAS-3** (6.77 ± 6.08 μM) < **MAAS-5** (9.12 ± 7.52 μM) < AZA (12.08 ± 2.00 μM) < **MAAS-4** (15.46 ± 8.65 μM); For hCA II: **MAAS-4**(1.09 ± 0.32 μM) < **MAAS-5** (2.01 ± 1.06 μM) < **MAAS-3** (6.49 ± 1.79 μM) < **MAAS-6** (17.65 ± 13.38 μM) < AZA (18.22 ± 4.90 μM) < **MAAS-7** (29.94 ± 0.82 μM). Both hCA I and hCA II have a higher K_i value than AZA, which is used as a standard in only one molecule. According to these data, it has been observed that these molecules have the potential to inhibit these enzymes.

CA inhibitors have been used in the treatment of various diseases such as AZA, brinzolamide (BRZ), topiramate, and methazolamide (MTZ) against CA I and CA II. These drugs are used in the treatment of glaucoma, epilepsy, migraine, and as diuretics. These systemically used drugs (AZA and MTZ) have side effects such as numbness, tingling in the fingers and toes, taste disturbance, blurred vision, and kidney stone formation.[50,51] The discovery of new compounds with fewer side effects and greater efficacy by researchers is one of the most studied topics in recent times.
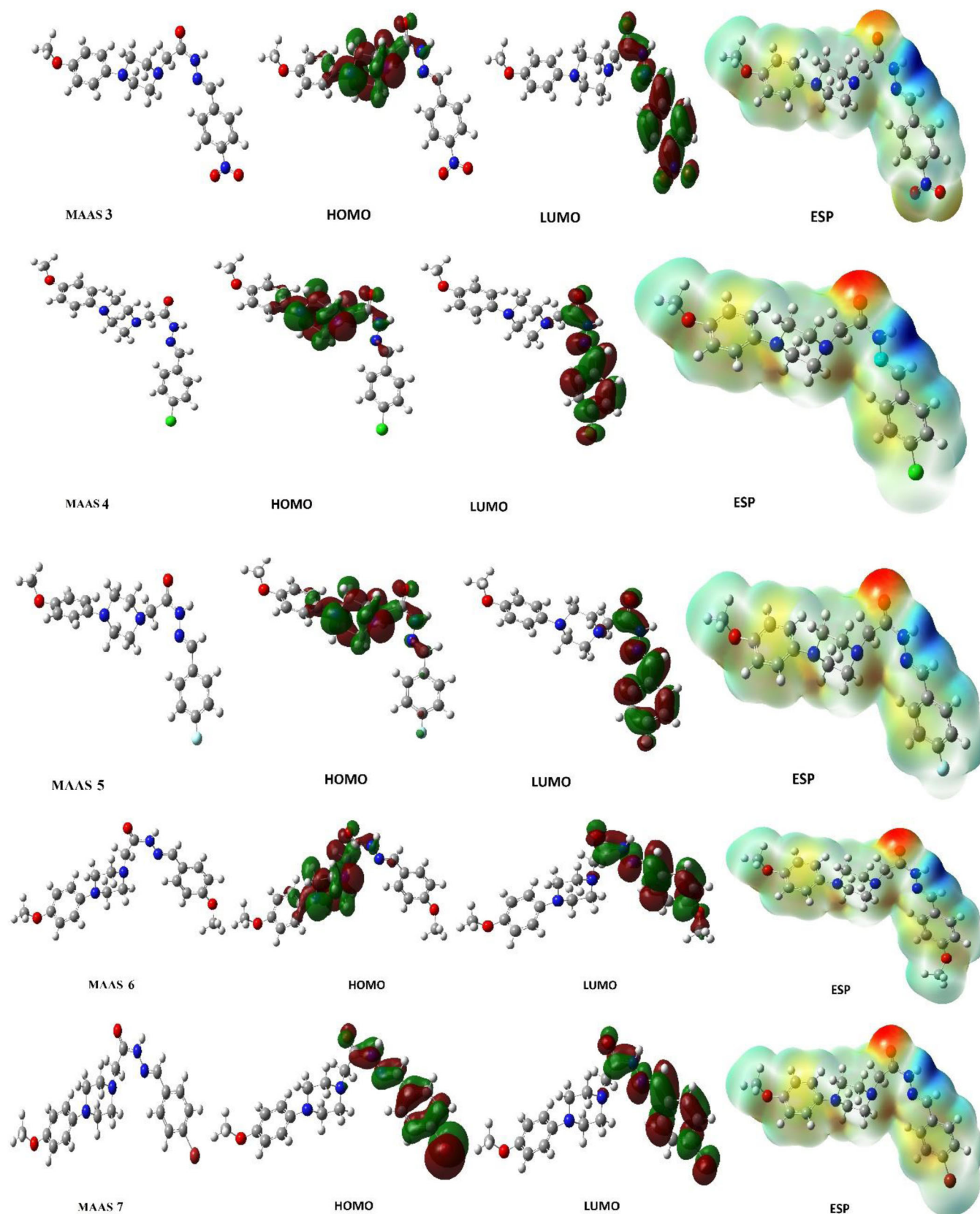
FIGURE 5 Shapes of optimized structure, Highest Occupied Molecular Orbital (HOMO), Lowest Unoccupied Molecular Orbital (LUMO), and electrostatic potential of all molecules.
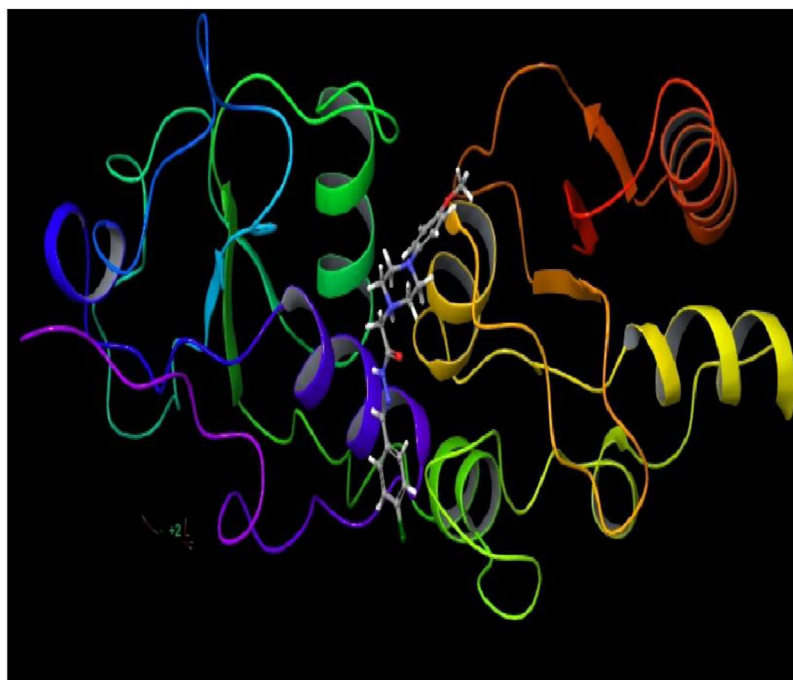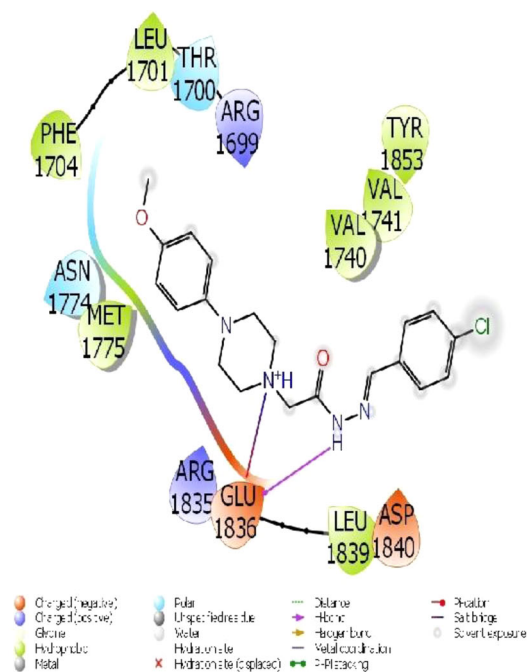
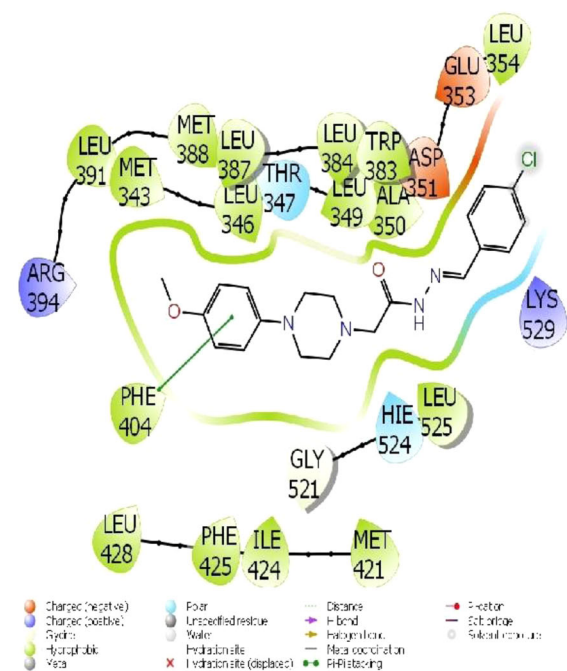**FIGURE 6** Presentation interactions of **MAAS-4** with 1JNX protein.

FIGURE 7 Presentation interactions of **MAAS-4** with 1A52 protein.

Epilepsy affects approximately 3% of the population at any time in life, with the highest incidence in childhood and the elderly. There is also a group of people (3%–6%) who are allergic to sulfur-based compounds and cannot be treated with sulphonamides. The data obtained from these studies showed that these molecules have new potential as carbonic anhydrase inhibitors.

3.7 | Theoretical calculations

The theoretical calculations were used to compare both the chemical properties of the compounds and their biological properties. It provided important information that had to be obtained before many experimental studies could be carried out. It
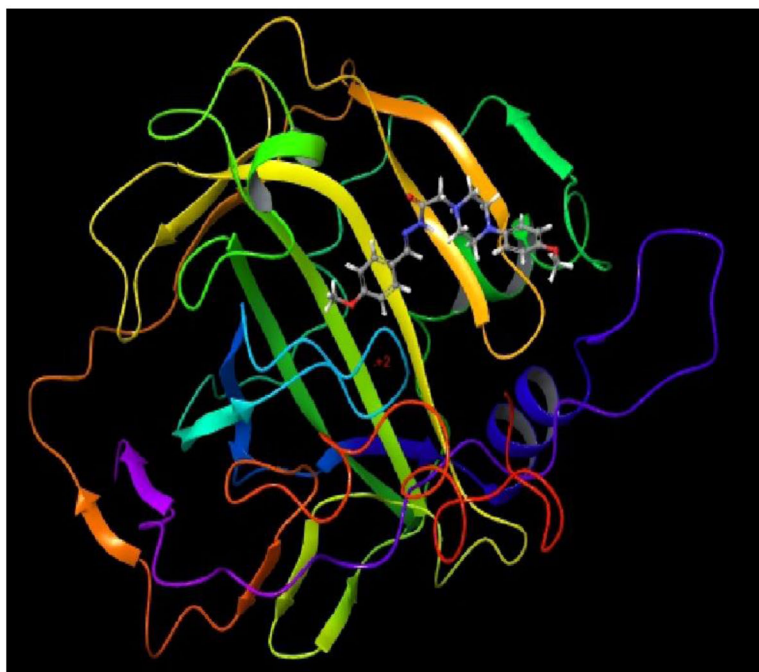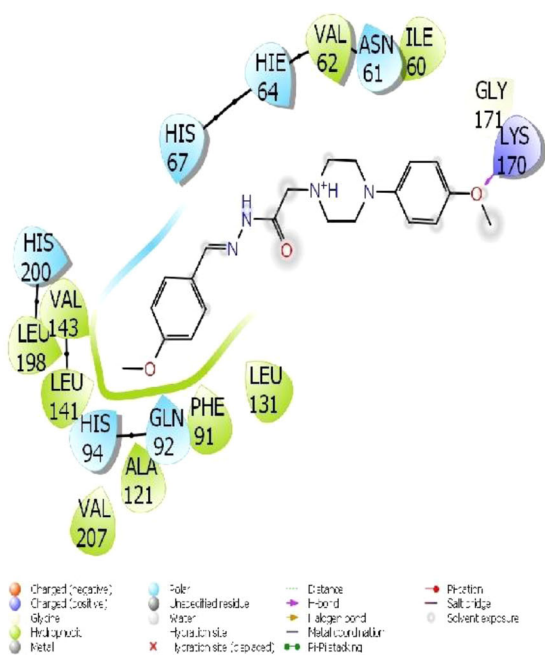
FIGURE 8 Presentation interactions of **MAAS-6** with human carbonic anhydrase I (hCA I) protein.
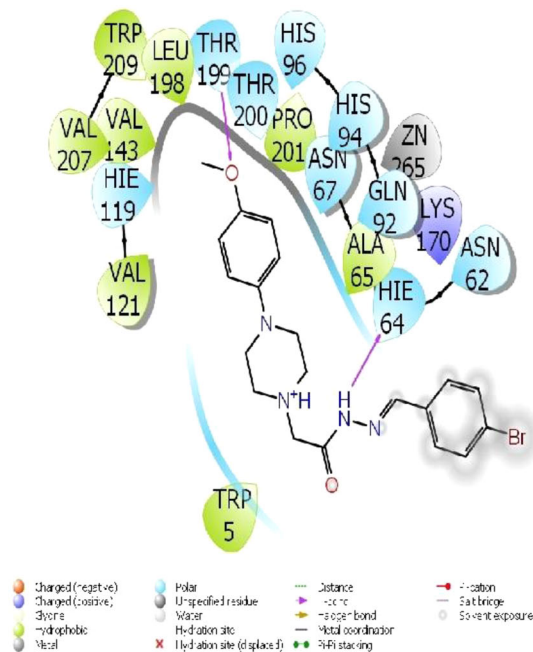

FIGURE 9 Presentation interactions of **MAAS-7** with human carbonic anhydrase II (hCA II) protein.

has important theoretical advantages in determining the active sites of molecules and in synthesizing more effective and active compounds.[52] Although many quantum chemical parameters are calculated in Gaussian calculations, the two most important parameters are HOMO (Highest Occupied Molecular Orbital), which shows the ability of compounds to donate electrons,[53] LUMO (Lowest Unoccupied Molecular Orbital), which shows the

ability of compounds to accept electrons.[54] All calculated parameters are listed in Table 6.

There are many parameters calculated in Table 6. Among these parameters, the ΔE energy gap value is another parameter that indicates the activity of the compounds. In general, it is known that when the numerical value of the HOMO parameter of the compounds is the most positive and the numerical value of the

TABLE 7 Numerical values of the docking parameters of molecules against enzymes.

	Docking Score	Glide ligand efficiency	Glide hbond	Glide evdw	Glide ecoul	Glide emodel	Glide energy	Glide einternal	Glide posenum
1JNX									
3	−3.16	−0.11	−0.36	−23.56	−8.66	−39.50	−32.21	3.30	381
4	−4.13	−0.12	−0.16	−26.02	−4.83	−37.60	−30.85	2.49	9
5	−3.16	−0.12	−0.36	−22.64	−7.23	−36.51	−29.88	4.37	108
6	−3.99	−0.14	−0.29	−22.26	−10.11	−42.48	−32.37	3.13	326
7	−3.21	−0.12	−0.08	−27.71	−4.61	−38.93	−32.31	3.11	9
1A52									
3	−6.11	−0.21	−0.16	−37.33	−7.82	−60.26	−45.16	6.91	54
4	−6.56	−0.17	0.00	−42.44	0.65	−35.77	−41.79	14.74	121
5	−4.85	−0.18	−0.08	−16.87	−5.40	−38.42	−22.26	11.82	4
6	−6.36	−0.23	−0.16	−34.81	−7.60	−56.87	−42.41	6.52	305
7	−3.68	−0.14	0.00	−37.63	0.85	−29.29	−36.78	17.20	166
2CAB									
3	−4.57	−0.16	−0.29	−33.96	−6.60	−50.94	−40.56	1.78	347
4	−4.48	−0.17	0.00	−36.92	−5.47	−53.49	−42.39	1.42	305
5	−4.79	−0.18	0.00	−36.70	−5.83	−54.09	−42.53	1.68	378
6	−4.81	−0.12	−0.16	−26.76	−1.74	−34.91	−28.50	1.61	373
7	−4.46	−0.17	−0.01	−38.03	−5.57	−54.76	−43.60	1.54	379
5AML									
3	−4.47	−0.16	−0.29	−33.84	−11.23	−52.33	−45.06	12.46	381
4	−3.81	−0.14	−0.13	−31.68	−5.84	−44.34	−37.52	3.67	137
5	−2.14	−0.08	−0.25	−31.92	−7.78	−46.89	−39.71	6.63	386
6	−1.06	−0.04	0.00	−35.78	−1.78	−40.76	−37.56	7.35	235
7	−5.17	−0.01	0.00	−34.45	−6.75	−50.19	−41.20	5.50	279

LUMO parameter is the most negative, the activity is the highest. Considering the explanations above, if the HOMO is the most positive and the LUMO is the most negative, the difference between them will be the smallest. This will increase the activity of the compounds. The compounds with the lowest ∆E energy gap have the highest activities.[53] One of the other parameters calculated is electronegativity, which indicates the strength of atoms in the molecule to attract bonding electrons.[54] The higher the numerical value of this parameter, the more the atoms in the molecule will attract the bonding electrons, reducing the activity of the molecules. Another parameter is the chemical hardness, which demonstrates the polarization property of molecules.[52] On the other hand, the opposite of chemical hardness is softness, and soft molecules are more reactive than hard molecules because they can easily donate electrons to an acceptor.

Although many parameters have been found as a result of theoretical calculations, very few of these parameters have figural representations. However, optimized shapes of the first visual compounds are given in Figure 5. The second and third figures show the HOMO and LUMO. In the last figure, the electrostatic potentials of the structures are given. There are red-colored regions which are electron-rich regions, on the visual compound. There are blue-colored regions, which are electron-poor regions, on the visual compound. These two regions are the active regions of the compound for both accepting and donating electrons.[52]

When the numerical values in Table 6 are examined, the compound **MAAS-6** has a higher activity due to its higher HOMO energy value than other compounds. However, the compound **MAAS-3** has a lower LUMO energy value than other compounds, and its activity is higher than other compounds. In the numerical value of another parameter, the DE energy value, it was observed that **MAAS-3** had a higher activity than other compounds because the numerical value of this parameter was lower. On the other hand, when the electronegative values of the compounds are examined, it is seen that the compound **MAAS-6** has a higher activity due to its lower electronegativity value. Considering the IC50 values in MCF-7

TABLE 8 ADME/T properties of the synthesized compounds.

	3	4	5	6	7	Reference range
mol_MW	397	387	370	382	431	130–725
dipole (D)	9.0	6.1	6.1	6.4	5.6	1.0–12.5
SASA	710	695	680	701	690	300–1000
FOSA	278	278	278	366	278	0–750
FISA	166	65	65	65	65	7–330
PISA	267	281	291	270	279	0–450
WPSA	0	72	47	0	69	0–175
volume (A^3)	1274	1244	1215	1270	1236	500–2000
donorHB	1	1	1	1	1	0-6
accptHB	7.3	6.3	6.3	7.0	6.3	2.0–20.0
glob (Sphere =1)	0.8	0.8	0.8	0.8	0.8	0.75–0.95
QPpolrz (A^3)	42.9	42.5	41.4	42.7	42.1	13.0–70.0
QPlogPC16	13.4	13.0	11.9	12.6	12.9	4.0–18.0
QPlogPoct	20.5	19.3	18.8	19.4	19.1	8.0–35.0
QPlogPC16	13.4	13.0	11.9	12.6	12.9	4.0–18.0
QPlogPoct	20.5	19.3	18.8	19.4	19.1	8.0–35.0
QPlogPw	11.4	10.1	10.1	10.5	10.0	4.0–45.0
QPlogPo/w	2.9	4.2	4.0	3.7	4.1	−2.0–6.5
QPlogS	−4.1	−4.6	−4.4	−4.1	−4.6	−6.5–0.5
CIQPlogS	−4.2	−4.4	−4.0	−4.0	−5.3	−6.5–0.5
QPlogHERG	−6.8	−6.8	−6.7	−6.6	−6.7	[a]
QPPCaco (nm/sec)	66	604	604	604	604	[b]
QPlogBB	−1.2	0.1	0.1	-0.1	0.1	−3.0–1.2
QPPMDCK (nm/sec)	29	787	572	317	753	[b]
QPlogKp	−5.0	−3.2	−3.2	−3.1	−3.2	Kp in cm/h
IP (ev)	8.5	8.2	8.2	8.1	8.2	7.9–10.5
EA (eV)	2.4	1.2	1.2	1.1	1.2	−0.9–1.7
#metab	4	3	3	4	3	1–8
QPlogKhsa	0.3	0.5	0.4	0.4	0.5	−1.5–1.5
Human Oral Absorption	3	3	3	3	3	-
Percent Human Oral Absorption	76	100	100	100	100	[c]
PSA	120	74	74	83	74	7–200
RuleOfFive	0	0	0	0	0	Maximum is 4
RuleOfThree	0	0	0	0	0	Maximum is 3
Jm	0.0	0.0	0.0	0.0	0.0	-

[a]corcern below −5.

[b]<25 is poor and >500 is high.

[c]<25% is poor and >80% is high.

and HeLa cell lines as a result of experimental procedures, it is seen that the activity of **MAAS-3** molecule is higher than other molecules. The results of the Gaussian calculations introduced that the activities of the compounds **MAAS-3** and **6** were higher in general.

After the Gaussian calculations, the activities of compounds against biological materials were investigated. The activities of the synthesized target compounds against prostate cancer protein, carbonic anhydrase I and II iszoenzymes (hCA I and hCA II) proteins were investigated. The most important thing that designates the activities of compounds is the chemical interaction that occurs between the compound and the target protein. These chemical interactions are hydrogen bonds, polar, hydrophobic interactions, pi–pi, and halogen.[55] The interactions between the studied proteins and compounds with each other are given in Figures 6–9. The parameters obtained from these interactions are given in Table 7.

As a result of the molecular docking calculations, the interactions of the compounds were observed. The most important ones among the parameters obtained afterwards are given in Table 7. These parameters give the numerical value of the chemical interactions (Glide hbond, Glide evdw, and Glide ecoul) that occur between compounds and proteins.[56] On the other hand, numerical values can be obtained about the poses (Glide emodel, Glide energy, Glide einternal, and Glide posenum) procured from the interaction of compounds with proteins.[55]

When the interactions were examined, it was seen that hydrogen bond interaction occured that the nitrogen atom in the formohydrazide group and the nitrogen atom in the piperazine ring in the compound **MAAS-4** with the GLU 1836 protein in the 1JNX protein in Figure 6. It was detected that Pi–Pi stacking interaction between the PHE 404 protein in the 1A52 protein and oxygen atom in the anisole ring group of the compound **MAAS-4** in Figure 7. Moreover, it was seen that hydrogen bond interaction between the nitrogen atom in the formohydrazide group in the compound **MAAS-7** and the HIE 64 protein in the hCA II enzyme protein in Figure 8. Also, the oxygen atom in the anisole group in the same compound made hydrogen bonds with the THR 199 protein in Figure 9.

The molecular docking results alone are not sufficient, because the results of molecular docking compare the theoretical activities of compounds, but do not recommend their use as a drug candidate. For this reason, ADME/T analysis was performed to predict the movements of compounds in human metabolism and to examine their effects and reactions in human metabolism in Table 8. With this analysis, the chemical and biological properties of the compounds were investigated. Many parameters such as molar mass of molecules (mol_MW), dipole moment (dipole), Total solvent accessible surface area (SASA), volume, donorHB (given hydrogen bond), accptHB (accepted hydrogen bond), Globularity descriptor (glob), Predicted polarizability (QPpolrz) were calculated.[57,58] Apart from these, to examine the biological properties of compounds, their movements in human metabolism have been tried to be predicted. Many parameters such as brain–blood (QPPMDCK) and intestinal–blood (QPPCaco) barriers of molecules, Predicted skin permeability (QPlogKp), and Number of likely metabolic reactions (#metab) were calculated.[57,58] Furthermore, two important parameters are violations of Lipinski's rule of five (RuleOfFive)[59,60] and violations of Jorgensen's rule of three (RuleOfThree)[59] were also found "0" for the compounds. The numerical value of this important parameter is required to be zero. When the numerical values of all the calculated parameters are examined, it has been found that there is no harm in the application of the target compounds to the human metabolism as theoretical drug candidates.

4 | CONCLUSION

The synthesized Schiff base derivatives were found to be effective to varying degrees in MCF-7 and HeLa cell lines. In addition, the synthesized compounds had cytotoxic effects on normal L929 cells as well as cytotoxic effects on cancer cells. Fibroblast cells are the primary target of many chemical agents. It should be investigated in further tests by examining the detailed anticarcinogenic activities of these compounds in other cancer cell lines and healthy cell cultures. Moreover, these compounds caused the increasing effect of antioxidant and oxidant load of the cells, but the important OSI was only observed in the MCF7 cell line. Therefore, they could be further investigated for their potential in obtaining and producing effective substances in the prevention of free radical-induced damage. The results of the interaction between the compounds and pBR322 show that the compounds **MAAS-4** and **5** at higher concentrations were able to induce moderate conformational changes in DNA. This is thought to be due to covalent interstrand binding. Furthermore, these two compounds are notable for their moderate antimicrobial activity, and it would be beneficial to investigate the effects on more microorganisms. The target compounds exhibited high inhibitory activities compared with standard inhibitors with K_i values in the range of 4.54 ± 0.86–15.46 ± 8.65 nM for hCA I (K_i value for standard inhibitor = 12.08 ± 2.00 nM), 1.09 ± 0.32–29.94 ± 0.82 nM for hCA II (K_i value for standard inhibitor = 18.22 ± 4.90 nM). Overall, these newly synthesized piperazine-incorporated Schiff base derivatives are potential metabolic enzyme inhibitors. Finally, as a result of the theoretical calculations performed, the activities of the compounds were compared with both DFT and molecular docking calculations. The results were found to be in great agreement with the experimental results. At the same time, the drug properties of the compounds were investigated. It was found that all compounds are theoretically free of any drawbacks for human metabolism. As a matter of fact, we think that these compounds could be future drug candidates, supported by various in vitro and in vivo studies.

ORCID
Arif Mermer http://orcid.org/0000-0002-4789-7180
Burak Tüzün http://orcid.org/0000-0002-0420-2043
Ümit M. Koçyiğit http://orcid.org/0000-0001-8710-2912

REFERENCES
[1] M. M. Poggi, C. N. Coleman, J. B. Mitchell, *Curr. Probl. Cancer* **2001**, *25*(6), 334.
[2] G. Wang, W. Liu, Z. Peng, Y. Huang, Z. Gong, Y. Li, *Bioorg. Chem.* **2020**, *103*, 104141.
[3] Ş. Comşa, A. M. Cîmpean, M. Raica, *Anticancer Res.* **2015**, *35*(6), 3147.
[4] R. G. Daré, C. V. Nakamura, V. F. Ximenes, S. O. S. Lautenschlager, *Free Radic. Biol. Med.* **2020**, *160*, 342.
[5] N. Takeyama, S. Miki, A. Hirakawa, T. Tanaka, *Exp. Cell Res.* **2002**, *274*(1), 16.
[6] M. F. Abo-Ashour, W. M. Eldehna, A. Nocentini, H. S. Ibrahim, S. Bua, H. A. Abdel-Aziz, S. M. Abou-Seri, C. T. Supuran, *Bioorg. Chem.* **2019**, *87*, 794.
[7] C. B. Mishra, M. Tiwari, C. T. Supuran, *Med. Res. Rev.* **2020**, *40*(6), 2485.
[8] a) A. Mermer, N. Demirbas, A. Colak, E. A. Demir, N. Kulabas, A. Demirbas, *ChemistrySelect* **2018**, *3*, 12234–12242.; b) A. Mermer, N. Demirbas, U. Cakmak, A. Colak, A. Demirbas, M. Alagumuthu, S. Arumugam, *J. Heterocycl. Chem.* **2019**, *56*(9), 2460–2468.
[9] A. S. El-Azab, A. A. M. Abdel-Aziz, S. Bua, A. Nocentini, M. A. El-Gendy, M. A. Mohamed, T. Z. Shawer, N. A. AlSaif, C. T. Supuran, *Bioorg. Chem.* **2019**, *87*, 78.
[10] P. Taslimi, U. M. Kocyigit, B. Tüzün, M. Kirici, *J. Biomol. Struct. Dyn.* **2022**, *40*(6), 2489.
[11] A. Bahadur, S. Iqbal, S. Muneer, H. O. Alsaab, N. S. Awwad, H. A. Ibrahium, *Bioorg. Med. Chem. Lett.* **2022**, *57*, 128520.
[12] A. Huseynova, R. Kaya, P. Taslimi, V. Farzaliyev, X. Mammadyarova, A. Sujayev, B. Tüzün, U. M. Kocyigit, S. Alwasel, İ. Gulçin, *J. Biomol. Struct. Dyn.* **2022**, *40*(1), 236.
[13] M. F. Abo-Ashour, W. M. Eldehna, A. Nocentini, A. Bonardi, S. Bua, H. S. Ibrahim, M. M. Elaasser, V. Kryštof, R. Jorda, P. Gratteri, S. M. Abou-Seri, C. T. Supuran, *Eur. J. Med. Chem.* **2019**, *184*, 111768.
[14] H. Gezegen, M. B. Gürdere, A. Dinçer, O. Özbek, Ü. M. Koçyiğit, P. Taslimi, B. Tüzün, Y. Budak, M. Ceylan, *Arch. Pharm. (Weinheim)* **2021**, *354*(4), 2000334.
[15] C. Türkeş, M. Arslan, Y. Demir, L. Çoçaj, A. Rifati Nixha, Ş. Beydemir, *Bioorg. Chem.* **2019**, *89*, 103004.
[16] M. Al-Qubaisi, R. Rozita, S. K. Yeap, A. R. Omar, A. M. Ali, N. B. Alitheen, *Molecules* **2011**, *16*(4), 2944.
[17] R. S. Williams, R. Green, J. N. M. Glover, *Nat. Struct. Biol.* **2001**, *8*(10), 838.
[18] D. M. Tanenbaum, Y. Wang, S. P. Williams, P. B. Sigler, *Proc. Natl. Acad. Sci.* **1998**, *95*(11), 5998.
[19] K. K. Kannan, M. Ramanadham, T. A. Jones, *Ann. N Y Acad. Sci.* **1984**, *429*, 49. https://doi.org/10.2210/pdb2cab/pdb
[20] J. Ivanova, J. Leitans, M. Tanc, A. Kazaks, R. Zalubovskis, C. T. Supuran, K. Tars, *Chem. Commun.* **2015**, *51*(33), 7108.
[21] H. Uslu, D. Osmaniye, B. N. Sağlik, S. Levent, Y. Özkay, K. Benkli, Z. A. Kaplancikli, *Bioorg. Chem.* **2021**, *117*, 105430.
[22] W. X. Sun, Y. J. Ji, Y. Wan, H. W. Han, H. Y. Lin, G. H. Lu, J. L. Qi, X. M. Wang, Y. H. Yang, *Bioorg. Med. Chem. Lett.* **2017**, *27*(17), 4066.
[23] S. Vanaparthi, R. Bantu, N. Jain, S. Janardhan, L. Nagarapu, *Bioorg. Med. Chem. Lett.* **2020**, *30*(16), 127304.
[24] J. Eloff, *Planta Med.* **1998**, *64*(08), 711.
[25] W. G. Lima, F. J. dosSantos, A. Cristina Soares, F. A. Macías, J. M. G. Molinillo, J. Maria Siqueira Ferreira, J. Máximo de Siqueira, *Synth. Commun.* **2019**, *49*(2), 286.
[26] O. Erel, *Clin. Biochem.* **2005**, *38*(12), 1103.
[27] J. Masternak, M. Zienkiewicz-Machnik, I. Łakomska, M. Hodorowicz, K. Kazimierczuk, M. Nosek, A. Majkowska-Młynarczyk, J. Wietrzyk, B. Barszcz, *Int. J. Mol. Sci.* **2021**, *22*(14), 7286.
[28] Ç. Boğatarkan, S. Utku, L. Acik, *Rev. Roum. Chim.* **2015**, *60*(1), 59.
[29] N. Gönül Baltaci, E. F. Koçpınar, H. Budak, *Mol. Biol. Rep.* **2021**, *48*(11), 7397.
[30] J. A. Verpoorte, S. Mehta, J. T. Edsall, *J. Biol. Chem.* **1967**, *242*(18), 4221.
[31] D. D. Armstrong, *New York Certified Public Accountant (pre-1986)* **1966**, *36*(000008), 573.
[32] A. H. Eldeeb, M. F. Abo-Ashour, A. Angeli, A. Bonardi, D. S. Lasheen, E. Z. Elrazaz, A. Nocentini, P. Gratteri, H. A. Abdel-Aziz, C. T. Supuran, *Eur. J. Med. Chem.* **2021**, *221*, 113486.
[33] M. J. Frisch, G. W. Trucks, H. B. Schlegel, G. E. Scuseria, M. A. Robb, J. R. Cheeseman, G. Scalmani, V. Barone, B. Mennucci, G. A. Petersson, H. Nakatsuji, M. Caricato, X. Li, H. P. Hratchian, A. F. Izmaylov, J. Bloino, G. Zheng, J. L. Sonnenberg, M. Hada, M. Ehara, K. Toyota, R. Fukuda, J. Hasegawa, M. Ishida, T. Nakajima, Y. Honda, O. Kitao, H. Nakai, T. Vreven, J. A. Montgomery, J. E. Peralta, F. Ogliaro, M. Bearpark, J. J. Heyd, E. Brothers, K. N. Kudin, V. N. Staroverov, R. Kobayashi, J. Normand, K. Raghavachari, A. Rendell, J. C. Burant, S. S. Iyengar, J. Tomasi, M. Cossi, N. Rega, J. M. Millam, M. Klene, J. E. Knox, J. B. Cross, V. Bakken, C. Adamo, J. Jaramillo, R. Gomperts, R. E. Stratmann, O. Yazyev, A. J. Austin, R. Cammi, C. Pomelli, J. W. Ochterski, R. L. Martin, K. Morokuma, V. G. Zakrzewski, G. A. Voth, P. Salvador, J. J. Dannenberg, S. Dapprich, A. D. Daniels, O. Farkas, J. B. Foresman, J. V. Ortiz, J. Cioslowski, D. J. Fox, *Gaussian 09, revision D.01*, Gaussian Inc, Wallingford CT **2009**.
[34] R. Dennington, T. A. Keith, J. M. Millam, *GaussView 6.0. 16*, Semichem Inc.: Shawnee Mission, KS, USA **2016**.
[35] A. D. Becke, *J. Chem. Phys.* **1992**, *96*(3), 2155.
[36] D. Vautherin, D. M. Brink, *Phys. Rev. C* **1972**, *5*(3), 626.
[37] E. G. Hohenstein, S. T. Chill, C. D. Sherrill, *J. Chem. Theory Comput.* **2008**, *4*(12), 1996.
[38] B. Tüzün, *Spectrochim. Acta, Part A* **2020**, *227*, 117663.
[39] B. Tüzün, *Turk. Comput. Theor. Chem.* **2018**, *2*(1), 12.
[40] A. Günsel, A. T. Bilgiçli, B. Tüzün, H. Pişkin, G. Y. Atmaca, A. Erdoğmuş, M. N. Yarasir, *J. Photochem. Photobiol., A* **2019**, *373*, 77.
[41] Schrödinger Release 2021-3, *Maestro, Schrödinger*, LLC, New York, NY **2021**.
[42] Schrödinger Release 2019-4, *Protein Preparation Wizard; Epik, Schrödinger, LLC, New York, NY, 2016; Impact, Schrödinger, LLC, New York, NY, 2016*, Prime, Schrödinger, LLC, New York, NY **2019**.
[43] Schrödinger Release 2021-3, *LigPrep, Schrödinger* **2021**, LLC. New York, NY.

[44] H. A. Alzahrani, M. M. Alam, A. A. Elhenawy, A. M. Malebari, S. Nazreen, *J. Mol. Struct.* **2022**, *1253*, 132265.

[45] Schrödinger Release 2021-3, *QikProp, Schrödinger*, LLC, New York, NY **2021**.

[46] S. Demirci, A. Mermer, G. Ak, F. Aksakal, N. Colak, A. Demirbas, F. A. Ayaz, N. Demirbas, *J. Heterocycl. Chem.* **2017**, *54*, 1785.

[47] A. Mermer, N. Demirbas, H. Uslu, A. Demirbas, S. Ceylan, Y. Sirin, *J. Mol. Struct.* **2019**, *1181*, 412.

[48] D. Wang, S. J. Lippard, *Nat. Rev. Drug Discovery* **2005**, *4*(4), 307.

[49] S. Utku, F. Gumus, S. Tezcan, M. S. Serin, A. Ozkul, *J. Enzyme Inhib. Med. Chem.* **2010**, *25*(4), 502.

[50] G. Bianco, R. Meleddu, S. Distinto, F. Cottiglia, M. Gaspari, C. Melis, A. Corona, R. Angius, A. Angeli, D. Taverna, S. Alcaro, J. Leitans, A. Kazaks, K. Tars, C. T. Supuran, E. Maccioni, *ACS Med. Chem. Lett.* **2017**, *8*(8), 792.

[51] A. Bonardi, A. B. Vermelho, V. da Silva Cardoso, M. C. de Souza Pereira, L. da Silva Lara, S. Selleri, P. Gratteri, C. T. Supuran, A. Nocentini, *ACS Med. Chem. Lett.* **2019**, *10*(4), 413.

[52] R. Y. Jin, C. Y. Zeng, X. H. Liang, X. H. Sun, Y. F. Liu, Y. Y. Wang, S. Zhou, *Bioorg. Chem.* **2018**, *80*, 253.

[53] Z. Yan, A. Liu, M. Huang, M. Liu, H. Pei, L. Huang, H. Yi, W. Liu, A. Hu, *Eur. J. Med. Chem.* **2018**, *149*, 170.

[54] A. Mermer, H. Bayrak, S. Alyar, M. Alagumuthu, *J. Mol. Struct.* **2020**, *1208*, 127891.

[55] A. Poustforoosh, H. Hashemipour, B. Tüzün, A. Pardakhty, M. Mehrabani, M. H. Nematollahi, *Biophys. Chem.* **2021**, *272*, 106564.

[56] S. Sahu, S. K. Ghosh, P. Gahtori, U. Pratap Singh, D. R. Bhattacharyya, H. R. Bhat, *Pharmacological Reports* **2019**, *71*(5), 762.

[57] L. M. Nainwal, M. Shaquzquzzaman, M. Akhter, A. Husain, S. Parvez, F. Khan, M. Naematullah, M. M. Alam, *Bioorg. Chem.* **2020**, *104*, 104282.

[58] C. A. Lipinski, *Drug Discovery Today: Technol.* **2004**, *1*(4), 337.

[59] C. A. Lipinski, F. Lombardo, B. W. Dominy, P. J. Feeney, *Adv. Drug Delivery Rev.* **1997**, *23*, 3.

[60] W. L. Jorgensen, E. M. Duffy, *Adv. Drug Delivery Rev.* **2002**, *54*(3), 355.